

January 01, 2009

## Size-based cell sorting by deterministic lateral displacement

Deepa Sritharan  
*Northeastern University*

---

### Recommended Citation

Sritharan, Deepa, "Size-based cell sorting by deterministic lateral displacement" (2009). *Chemical Engineering Master's Theses*. Paper 8.  
<http://hdl.handle.net/2047/d10019078>

This work is available open access, hosted by Northeastern University.

**SIZE-BASED CELL SORTING BY  
DETERMINISTIC LATERAL DISPLACEMENT**

A Thesis Presented

By

Deepa Sritharan

To

The Department of Chemical Engineering

In partial fulfillment of the requirements

For the degree of

Master of Science

In the field of

Chemical Engineering

Northeastern University

Boston, Massachusetts

January 27, 2009

## ACKNOWLEDGEMENT

I have been fortunate to work under the able supervision of my advisor Shashi K. Murthy who introduced me to the field of microfluidics. I am grateful to him for permitting me to work on this project and for offering his thoughtful guidance and support. I am indebted to the members of the BioMEMS Resource Center at the Massachusetts General Hospital who were extremely generous in taking time off from their busy schedules to share their knowledge and experience with me in designing my experiments. I am grateful to Scott McNamara and Praba Selvarasah for their valuable assistance with the microfabrication equipment at the George J. Kostas Nanoscale Technology and Manufacturing Research Center at Northeastern University. I also cherish the input by Joscelyn Harris and Priston Blackett from the Health Careers Academy who helped me with testing the microfluidic devices. I am thankful to my colleagues Brian Plouffe and Anilkumar Achyuta for their camaraderie and help. I owe much to my friends and classmates who offered encouragement and buoyed me up when I needed it most. I am grateful to Professor Behrooz Satvat for his valuable advice and moral support throughout my stay at Northeastern. I thank Dr. Rifat Sipahi and Dr. Rebecca Carrier for taking time to read and evaluate my thesis.

I am grateful to the Department of Chemical Engineering at Northeastern University for their financial assistance during my graduate studies.

I am indebted to my family for their unrelenting belief in my capabilities, love and counsel, on which I have relied on at every turn of the road, to stay focused. I dedicate this thesis to them.

## **ABSTRACT**

Microfluidic devices offer several advantages over conventional, large scale cell sorting systems. Creating microfluidics technology for lab-on-a-chip adaptations of these systems provides several benefits: simplicity of operation, improved transport control, portability, greater accessibility, reduced cost and potential for integration with other analytical techniques. This technology supplies important tools for biomedical applications such as tissue culture, drug discovery and point-of-care diagnostic systems.

This work presents a microfluidic device which uses asymmetric bifurcation of laminar flow around objects for the continuous separation of cell subpopulation from a heterogeneous cell suspension. Based on their size, each cell chooses its path through the device deterministically. Thus theoretically, all cells of the same size would follow the same path resulting in high resolution. This study investigates the effect of various design parameters on the performance of the microfluidic chip using experimental methods.

The microfluidic devices were manufactured from poly(dimethyl) siloxane (PDMS) using patterned silicon wafers by replica molding. Experiments were conducted using spherical mammalian cells and the cell movement was observed under a microscope. The cell movement within the device was disrupted repeatedly during the experiments because of cell clumping and the flexible nature of the cells. Nevertheless, the cells were observed to be laterally displaced and fractionation of the input sample was observed.

# TABLE OF CONTENTS

LIST OF FIGURES .....	v
1.0 INTRODUCTION.....	1
2.0 LITERATURE REVIEW.....	5
2.1 Sieve-Based Microfluidic Cell Separation.....	12
2.2 Lateral Displacement of Cells using Microfluidics .....	16
3.0 EXPERIMENTAL .....	21
3.1 Materials.....	21
3.2 Photolithography.....	22
3.2.1 <i>Making the Photomask</i> .....	22
3.2.2 <i>Photoresist Application</i> .....	22
3.2.3 <i>Exposure and Developing</i> .....	23
3.3 Soft Lithography .....	24
3.3.1 <i>Properties of PDMS</i> .....	27
3.3.2 <i>Surface Functionalization</i> .....	28
3.4 Cell Culture .....	29
4.0 RESULTS AND DISCUSSION.....	30
4.1 Wafer Fabrication .....	30
4.2 Preparing the Cell Suspension.....	32
4.3 Flow Experiments.....	32
4.4 Device Design.....	33
4.5 Problems Encountered During Flow Experiments.....	43
4.5.1 <i>PDMS Debris</i> .....	43
4.5.2 <i>Cell Stiction</i> .....	43
5.0 CONCLUSIONS.....	47
6.0 RECOMMENDATIONS.....	48
7.0 REFERENCES.....	50

## LIST OF TABLES AND FIGURES

Table 1:	Widely-used conventional methods of cell sorting and their shortcomings, classified based on the distinguishing cell property exploited for the process of separation. Table 1(a): methods that separate cells based on their physical properties. Table 1(b): methods that apply a physical force field to separate cells based on non-specific surface properties. Table 1(c): common techniques that separate cell populations based on specific biomarkers present on the cell surface.....6	6
Figure 1:	Size-based cell separation using a sieve having a series of channels of successively smaller width.....12	12
Figure 2:	Sieve-based cell sorting device.....14	14
Figure 3:	Staggered layout of obstacles in microfluidic device for size-based cell separation by deterministic lateral displacement.....17	17
Figure 4:	Asymmetric bifurcation of spherical particles: size based separation where a stream of fluid flows perpendicular to a series of obstacles of defined size and spacing. The flow is confined to one of three fluid streamlines. Particles smaller than the streamline width, zigzag between the obstacles. Larger particles collide with the obstacles and get displaced only in one direction, allowing for separation to occur.....18	18
Figure 5:	Replica molding with PDMS.....26	26
Figure 6:	Side view of a portion of the cylindrical post array used in microfluidic cell sorting post device.....26	26
Figure 7:	Tapered structures formed due to insufficient exposure to UV radiation...31	31
Figure 8:	Initial device design.....34	34
Figure 9:	Device design with modified inlet for hydrodynamic focusing of sample..34	34
Figure 10:	H1975 cell concentration at each outlet. Outlet “1” is the bottom-most outlet and outlet “7” is the top-most outlet. An inlet concentration of $0.5 \times 10^6$ cell/mL was injected into the device. Cells were focused to outlet “5” illustrating lateral displacement of target cells. Error bars denote standard errors for each point based on ten repetitions.....35	35

Figure 11: The maximum concentration of cells was determined to be in the fifth position. These results illustrated the ability of this device design to focus the cells to position “5”. It was determined by visual inspection that the displacement of the cells was occasionally hindered by the adhesion of cells between posts causing the streamline fluid flow to be displaced and thus the “bumping” of particles to be unpredictable and random.....

36

Figure 12: Device design using two separation zones- larger posts are followed by smaller posts downstream.....

36

Figure 13: H1975 cell fractions collected by using the device shown in figure 11 showed that the performance was significantly affected by the obstruction at interface. Error bars denote standard errors for each point based on three repetitions.....

37

Figure 14: Final device design consisted of a longer separation zone to maximize the area available for cell movement.....

38

Figure 15: Plot showing the size distribution of H1975 cells collected in each of the seven outlets. Error bars denote standard errors for each point based on ten repetitions.....

39

Figure 16: Plot showing the size distribution of A7r5 cells collected in each of the seven outlets. Error bars denote standard errors for each point based on three repetitions.....

40

Figure 17: Plot showing the size distribution of H5V fractions. Error bars denote standard errors for each point based on two repetitions.....

40

Figure 18: Plot showing the size distribution of a 1:1 mixture of H1975 cells and 3T3-J2 cells collected in each of the seven outlets. Error bars denote standard errors for each point based on two repetitions.....

41

Figure 19: Size distribution of the cell fractions collected from seven outlets in a run conducted using H5V cells.....

42

Figure 20: Cell stiction disrupts flow pattern of cells.....

44

Figure 21: Cell agglomeration causes smaller cells to form a larger unit and thus shifts the flow path away from the expected streamline.....

45

Figure 22: Microscope image showing cell agglomeration near the entrance.....45

Figure 23: Reverse displacement- cells are often disposed to move both ways around an obstacle.....46

## 1.0 INTRODUCTION

Cell separation devices play a central role in life science research for the analysis and processing of biological materials. Conventional systems used to perform these analyses have restricted accessibility due to the complexity of equipment and their high maintenance and operational costs. The patient sample must be moved to a laboratory and skilled technicians are often required to operate the instrumentation. Point-of-care diagnostic systems could greatly ease the burden of catering to the ever-increasing healthcare demands as they do not require trained professionals for operation. They can be easily fabricated for performing routine analytical procedures that are affordable, easy to use and yet give fast and reliable results. Microfluidics has the immense potential to create integrated, portable clinical diagnostic devices for point-of-care applications by executing time-consuming laboratory procedures at a microscale on a single chip. Microfluidic devices can be useful for tissue culture applications (where donor samples are scarce) and in the processing of whole blood samples, bacterial/mammalian cell suspensions, and protein/antibody solutions [1]. The development of microfluidic devices for rapid and inexpensive processing of samples is burgeoning in fields such as cancer and immunology research, drug testing and drug delivery, protein analysis by mass spectrometry, DNA analysis, cell manipulation, cell sorting, and cell patterning [2-7].

The miniaturization of bio-analysis systems offers several benefits over conventional macroscale technologies. A large number of portable, disposable and biocompatible microfluidic devices can be quickly manufactured cost-effectively by means of rapid prototyping. The operation of these devices can be efficiently automated

to achieve high-speed processing using only small amounts of chemical reagents and patient samples for analysis. Microfluidic device substrates can be fabricated by modifying conventional lithographic methods of silicon micromachining [8]. Microfabrication techniques offer great design flexibility as assay operations can be integrated with sample preparation and processing on the same chip. As these devices can perform continuous and real-time testing of samples, these devices could find an important place in detecting biochemical agents and pathogens in water or air samples.

Miniaturization begins with creating the basic microfluidic chip which consists of a network of microchannels connecting a series of fluid reservoirs. The microfluidic elements can then be connected with miniaturized sensors, on-chip analysis tools, and automated control units to form a lab-on-a-chip device or micro total analysis system ( $\mu$ TAS) [8]. Several physical phenomena that occur at the microscale can be exploited for driving fluids or manipulating particles such as pressure forces, electric fields magnetic fields, capillary forces, centrifugal forces, and optical forces [9]. It is possible to radically improve the sensitivity of analysis by shrinking the dimensions of the separating device to those of the species being analyzed. Decreasing the characteristic length scale reduces the time scale, resulting in quicker sample processing. This makes it possible to achieve a faster diagnosis and thereby facilitates quicker medical intervention.

Two broad areas where microfluidic tools would be useful are in medical diagnostics and tissue engineering. For example, in combating diseases such as cancer which are characterized by changes in cell morphology or specific cell surface markers [10], these devices can be used for rapid diagnosis in the early stages of the disease. In all tissue engineering applications, cell sorting is the primary step. Digested donor tissue

suspension can be enriched for specific cell types by running it through a microfluidic cell-sorting device to rapidly provide purified cell populations for tissue culture.

Several variations of microfluidic cell sorters, implementing different sorting mechanisms, have been designed and fabricated. The method of cell isolation is selected based on the nature of the application. Several strategies exist for the separation of different cell types in microfluidic devices, based on specific cell characteristics. Size-based separation techniques involve creating various geometries that guide different sized cells along specific routes. Adhesion-based microfluidic cell separation involves creating functionalized micro-channel surfaces that bind to specific cell receptors and entrap the cells of interest. Alternatively, cells can also be tracked by selectively attaching magnetic/fluorescent tags.

After a suitable method of isolation has been decided upon, preliminary evaluations of the design components are made by using numerical models that predict the particulate flow patterns within the device. Experiments are performed in conjunction with developing the numerical model in order to identify the factors that influence microfluidic chip operation which are not represented in numerical simulations. The theoretical design is then iterated by incorporating these factors and the modified version of the device is tested experimentally. The key challenge in developing the microfluidic sorting device is to design several such experiments in conjunction with a numerical model which closely simulates the functioning of the device.

Currently, the cell cytometry is one of the most commonly used methods to characterize cell populations by single cell analysis methods. The cytometer can be combined with a fluorescence-activated cell sorter (FACS), to enrich selected

subpopulations [11]. Apart from requiring sizable sample quantities, the problem with existing flow cytometers is that the time needed to process the signal data limits the rate at which cells can be detected. The use of a cell sorting element will be critical in many lab-on-a-chip devices, where cell detection or population enrichment is required prior to analysis.

This thesis examines the design and operation of a microfluidic device to separate a heterogeneous mixture of cells, based on their size. It uses a technique called “deterministic lateral displacement”, first described by Huang et al [12] to continuously separate a stream of differently sized particles. At low Reynolds numbers, when particles flow past an array of obstacles, they follow different predetermined paths depending on their size. The obstacles are cylindrical posts arranged to bifurcate the flow asymmetrically at a fixed angle with respect to the inlet stream. The principal parameter that decides the device design is the critical diameter. Particles larger than the critical diameter follow a path determined by asymmetric bifurcation of flow, while particles smaller than the critical diameter follow the streamline along the walls of the obstacles.

This work aims to describe the steps involved in developing a disposable and inexpensive microfluidic cell sorting device that requires no *a priori* knowledge of cell-specific markers or proteins to achieve separation. Hence this approach can be used to identify cells that do not express known markers, such as progenitor cells and other rare cells. Since the devices do not contain any biological markers or proteins, this technique allows the rapid manufacture of several devices that have a long shelf life.

## 2.0 LITERATURE REVIEW

Microfluidic devices are recently finding widespread application in the isolation of pure cell populations from heterogeneous suspension in both clinical and basic biomedical research. Microfluidic devices have the ability to handle a large number of small samples with high sensitivity. Designing microfluidic detection modules obviates the need for bench-top analyzers, making self-sufficient devices for point-of-care diagnostics when simple positive/negative results are sought. This section reviews some of the current literature in microfluidic research.

Microfluidics is finding increasing application in areas such as DNA microarray screening [13] and in understanding single-cell behavior [14]. With advances in stem cell biology, the isolation of rare cells has become an active area of research. Islet 1+ cells that are cardiac progenitor cells are present in very small numbers- 100 islet 1+ cells among  $10^9$  heart cells [15]. Currently, progenitor cells are isolated by pre-plating the heart cell suspension for 1 hour, after which fibroblasts and some islet 1+ cells remain attached to the tissue culture plastic. After 4-6 days in culture, the progenitors make up only 0.5% of the total cell population found in the plates [15]. Development of robust and efficient methods for isolating rare cells would be a major contribution to stem cell biology.

The diagnostic test for HIV infection relies on the separation of human lymphocytes from whole blood [16]. An enormous global effort is being made to bring antiretroviral treatment to infected people. While drug prices have dropped considerably, the cost and technical complexity of the test essential for the management of the HIV disease, such as CD4 cell counts remain prohibitive. Rodriguez et al describe a microfluidic device wherein fresh blood samples were stained with fluorescent

antibodies. The cells were captured on a membrane and the CD4 cells were counted by applying a computer algorithm that converts the digital image into CD4 counts real-time.

The method of cell isolation is selected based on the specific application. Some of the criteria used to determine the appropriate isolation technique for a given application are:

- the characteristic/feature that distinguishes the cell types
- the sample size available for analysis
- the required purity of the separated population with desired characteristics
- time taken for the complete cell separation process
- the total number of cells lost during the process of separation
- the viability of cells after separation
- the physical stress endured by the cells during the process
- the cost-effectiveness of the technique.

The following tables enlist some of the conventional cell separation methods and their shortcomings. Cells can be separated based on their physical attributes, non-specific surface properties or cell-specific surface properties.

**Table 1 (a)**

<b>Distinguishing Cell Physical Attribute</b>	<b>Separation Technique</b>	<b>Shortcomings</b>
Density	Centrifugation	Requires <i>a priori</i> knowledge of the density of the target cell-type and a solution capable of generating a density gradient must be used as

		the medium. Involves high maintenance costs, heat production, and protein denaturation. The technique relies on density rather than size differential and often results in incomplete separation.
Size	Cell strainers [17-20]	Cells tend to clog in the mesh filter. It is difficult to recover cells that have been retained on the mesh for cell culture. The technique is non-systematic as there are no parameters to control the process of separation.
Morphology	Flow cytometry	Needs a large number of cells for analysis. The time needed to process the signal data limits the rate at which cells can be detected. [21].

**Table 1 (b)**

<b>Non- Specific Cell Surface Property</b>	<b>Separation Technique</b>	<b>Shortcomings</b>
Hydrophobicity	Aqueous two-phase separation	Time consuming and needs expensive, high-purity dextrans [22].
Electrical charge	Electrophoresis	The process is time-consuming. Sample loading requires skill. The viability of cells is

		limited by electro-osmotic flow and temperature effects within the system [23]
--	--	--

**Table 1 (c)**

<b>Specific Cell Surface Property</b>	<b>Separation Technique</b>	<b>Shortcomings</b>
Surface markers	Pre-plating [24]	There is no means of controlling non-specific adhesion. There are no parameters that can be manipulated to control the process of separation. Adhered cells cannot be easily recovered and their viability is severely affected. In order to separate the cells with a lower concentration out of the cell suspension, they must be allowed to proliferate until they can be effectively isolated. Thus, it may take several days before the cell types are separated resulting in increased risk of changes in gene-expression.

	Fluorescence-activated cell sorting [17-20] Magnetic cell sorting	These are efficient but expensive methods [25]. Pre-processing is needed to attach various tags (fluorescent dyes, magnetic beads, etc.) onto cell surfaces. Prior knowledge of cell surface markers is required.
--	--	---

**Table 1: Widely-used conventional methods of cell sorting and their shortcomings, classified based on the distinguishing cell property exploited for the process of separation. Table 1(a) lists methods that separate cells based on their physical properties. Table 1(b) lists methods that apply a physical force field to separate cells based on non-specific surface properties. Table 1(c) lists common techniques that separate cell populations based on specific biomarkers present on the cell surface**

The limitations of the existing methods of separation described above motivate the development of more efficient cell separation techniques. The best compromise must be made between the speed of separation and the purity of the separated fractions. Separation technologies are required that are not only high fidelity in terms of identifying and isolating rare populations, but are also on a scale large enough to deliver adequate numbers of cells for rapid and clinically effective regeneration. The most significant advantage of microfluidic cell separation techniques over macroscale methods is for isolating rare cell populations. Microfluidics is useful in biomedical applications where a

highly specific separation is required. The amount of sample and reagent required for analysis is small. Due to the small scale of operation, several different processes can be integrated efficiently. Blood sampling is an area where microfluidics could make a significant contribution [26]. Blood contains substantial information about the functioning of tissues and organs in the body. Most laboratories still handle blood manually, in conditions that may significantly alter the results of subsequent analysis [26-28]. Microfluidic systems can drastically reduce such errors by decreasing the time between blood collection to analysis and by enabling sample analysis at the place where the blood is collected resulting in a more rapid and comprehensive analysis technique. Microfluidic devices, when used for experiments in small-animals, would require only minute amounts of blood for analysis, thus allowing sampling at multiple time points while causing the animal minimum adverse effects due to blood drawing [26].

Microfluidics can be used to separate target cells from a suspension by precise control and manipulation of fluids that are constrained to microscale geometries. Some of the control parameters include flow rate and device dimensions, shear stress and surface characteristics of the device walls. These devices are fabricated using lithography techniques originally developed in the semiconductor industry [15]. Several microfluidic devices can be cost-effectively fabricated in a short period of time by soft lithography technologies such as micro-contact printing, replica molding, microtransfer molding, micromolding in capillaries and solvent-assisted micromolding [29]. During micro-contact printing, a degassed elastomeric polymer (typically poly (dimethyl siloxane), PDMS) is poured onto a lithographically patterned mold, cured and then peeled off. The patterned polymer is then bonded to glass slides to create functional fluidic devices [30].

Thus polymers such as PDMS can be used for the inexpensive and rapid prototyping of microfluidic systems. While silicon is still an important micromachining material, polymers such as SU-8 and PDMS are finding widespread usage due to the ease of fabrication of devices with them. They have desirable physical properties such as optical transparency, thermal and electric insulation and low Young's modulus [31]. It is also easier to create integrated microfluidic devices (multilayered, multifunctional) using PDMS, as PDMS components can be securely sealed directly, while silicon-to-silicon connections require polymeric gaskets [31].

Several unique microfluidic separation techniques are being integrated into microscale and nanoscale fluidic devices. These devices are compact and simple. They are extremely effective for low throughput small-scale applications. Numerous microfluidic technologies developed in the recent years are approaches based on size, dielectric force and adhesion.

Adhesion-based cell separation systems are akin to chromatography columns where a mixture is passed through a column packed with functionalized beads or other materials capable of binding to the selected constituents of the feed. This method is used to separate cell populations that have well-defined surface markers or which require tagging because of a uniform size and/or density distribution, such as subpopulations of human lymphocytes [15]. However, as in FACS and MACS, these systems also require prior knowledge of cell surface markers.

In most size-based approaches, the device forces a fluid containing a heterogeneous cell population through channels or obstacles of varied dimensions. Unlike macroscale size-based separation approaches, the microscale geometry of the flow

channels results in low Reynolds numbers. This results in predictable and reproducible cell movement by laminar fluid flow. The main advantage of the size-based approach is that it does not require the presence of cell-specific markers or proteins to achieve separation. Hence this approach can be used to cells rare cells that do not express known markers. Furthermore, since the devices do not contain any biological markers or proteins, they have long shelf-lives and are easily transportable.

## 2.1 Sieve-Based Microfluidic Cell Separation

Mohamed et al [32] have designed a size-based separation device to isolate rare cells, such as metastatic cancer cells, from peripheral blood. The device comprised of an array of parallel conduits; each row consisted of more closely placed channels than the preceding row starting from 20  $\mu\text{m}$  and narrowing down to 2.5  $\mu\text{m}$  in width.

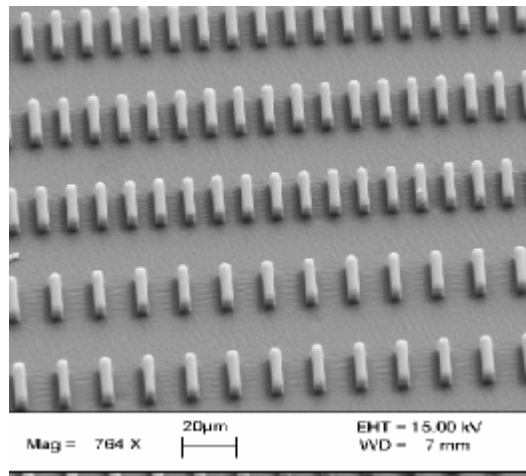


**Figure 1: Size-based cell separation using a sieve having a series of channels of successively smaller width. Flow is parallel to the channels [32]**

The chamber functions like a sieve, trapping larger cells such as mononuclear cells and neuroblastoma cells upstream in the larger channels, and allowing smaller cells such as erythrocytes to pass through. Several designs were investigated with varied

channel widths and heights before identifying the key dimensions required to trap the target cells. The channel width and height were dictated by the dimensions of the larger, rare cells (in this case, neuroblastoma cells or mononuclear cells). The smaller cells (erythrocytes) that formed the bulk of the sample continuously passed through unhindered by the sieve device. The trapped large cells were then removed from the device by flushing the cells from the outlet. Thus, the approach can only be applied to separate mixture of two cell types with significant differences in their dimensions.

PDMS and polyurethane were used for inexpensive fabrication of the device by micro-contact printing. When cultured neuroblastoma cells were mixed with either plain culture medium or peripheral blood and passed through the device, the larger neuroblastoma cells were consistently retained in the 10 $\mu$ m-wide, 20 $\mu$ m-deep channels while erythrocytes traversed through the device completely. Similarly, mononuclear cells in a sample of whole blood were trapped in 2.5 $\mu$ m-wide, 5 $\mu$ m-deep channels. While the technique is limited due to non-specific cell adhesion to the channel walls, the technique is more effective in terms of cost and time than conventional cell sorting techniques such as FACS or MACS.

Another sieve-based technique was described by Sethu et al [33]. They devised a microfluidic diffusive filter for continuously fractionating blood into its components. This device was applied for carrying out leukapheresis, to selectively deplete the blood of leukocytes. Leukapheresis is done before blood transfusion to prevent white blood cells from the donor from being transferred to the patient. This device employs micro-sieves that exploit the size and shape difference between the different cell types to remove leukocytes from whole blood. The device consisted of a middle channel (50  $\mu$ m wide,

200  $\mu\text{m}$  tall, and 4 cm long) connected to adjacent side channels by the micro-sieves (80  $\mu\text{m}$  wide, 5  $\mu\text{m}$  tall and 40  $\mu\text{m}$  in length). The side channels widened along the length of the device, ensuring constant pressure gradient across all sieves. The volumetric flow through each element of the sieve depends on pressure gradient (a function of the syringe pump controlled flow rate) and the fluidic resistance (constant for a given geometry). For small flow rates (up to 5  $\mu\text{l}/\text{min}$ ), the size and geometry of erythrocytes allow them to pass through the sieves unobstructed whereas leukocytes are larger and cannot pass through. At higher flow rates the pressure gradient across the filter elements of the sieves becomes large enough to support the passage of smaller leukocytes. Therefore if a cell encounters a sieve element and cannot pass through it is pushed along the main channel to the outlet due to the flow in the main channel. For this particular device design, at flow rates greater than 5  $\mu\text{l}/\text{min}$ , the pressure gradient across the filter elements becomes large enough to deform and force some of the leukocytes through into the diffuser.

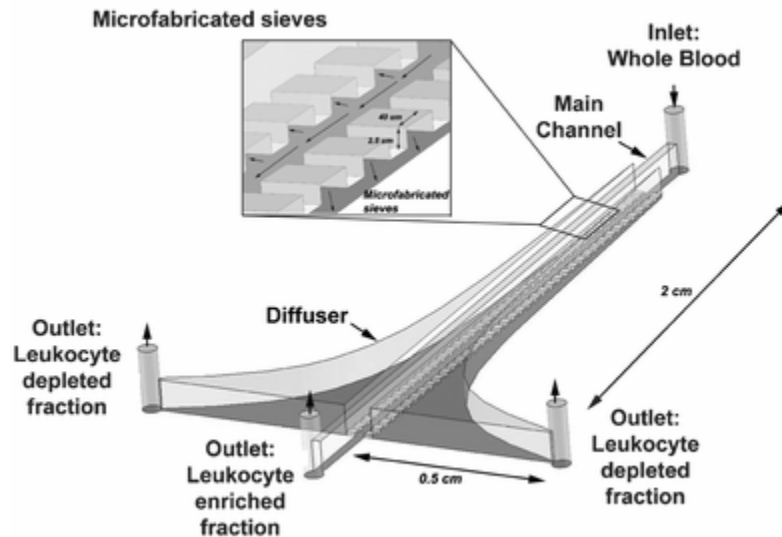


Figure 2: Sieve-based cell sorting device [33]

Murthy and coworkers applied this sieve-based approach to separate myocytes and non-myocytes from neonatal rat myocardium suspensions [34]. In contrast to the device developed by Mohamed et al, no cells were trapped in order to attain separation, rather the cells were separated according to the cells' ability to pass through the sieve.

The cell suspension diameter distribution from the middle-channel outlet and side-channel outlets were compared, and there was a statistically significant collection of the larger cells in the middle outlet versus the side outlets. Also the cells were shown to maintain viability, a common problem with size-based techniques. These results demonstrated the feasibility of a sieve-based approach to cell separation, on the basis of size. However, this technique again, separates the input sample into only two fractions. The other limitation was significant adhesion of both target and non-target cells, causing obstruction of numerous sieve devices. The results of Mohamed et al and Murthy et al illustrate the need to reduce the undesirable adhesive properties of device by modifying the surface and/or by optimizing the flow properties. Also this size-based separation technique is prone to clogging with particles or cells that are larger than the sieve size. Clogging can drastically reduce the efficiency of a flow-based separation process.

Other methods by which particles in solution are usually separated are by size-exclusion chromatography or hydrodynamic chromatography [12]. In the exclusion technique, a sample mixture stream flows through a tube packed with porous beads. Particles smaller than the pore size enter the beads and thus have longer migration path. Therefore the smaller particles are eluted out later than the larger particles [12, 35]. The problem with this technique is that, each particle within a certain size range may take different paths and thus get eluted at a time different from that expected. The multipath

effect reduces the resolution of this technique [12]. In hydrodynamic chromatography, the sample mixture is driven through a capillary by hydrodynamic flow. The fluid carrying the particles has a parabolic flow profile [12]. The large particles cannot intercept the boundary layer fluid near the capillary walls and thus move faster with the bulk of the fluid while the smaller particles are slowed down by the boundary layer forces. Multipath effects again limit separation resolution with this technique as it is difficult to predict and control the varying particle velocities in the parabolic flow [12, 36]. Devices mimicking both these techniques have been miniaturized using microfabrication technologies. In all of these devices however, a given size zone may have different migration paths and diffusion is required for separation. The separation technique of deterministic lateral displacement was demonstrated by Huang et al to create equivalent migration paths for each particle in a mixture, eliminating multipath zone broadening. This approach is elucidated below.

## **2.2 Lateral Displacement of Cells using Microfluidics**

This concept was established by Huang et al [12] for the size-based separation of polymer microspheres ranging in size between 0.8 and 1.0  $\mu\text{m}$  as well as circular plasmid DNA. The rectangular obstacles used in the initial model were replaced by circular cylinders [35] to improve the flow profile and prevent flow separation at the corners.

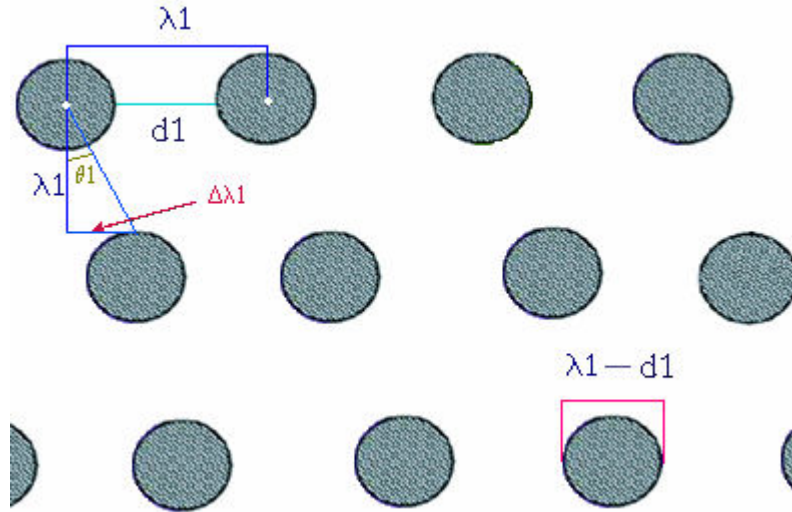


**Figure 3: Staggered layout of obstacles in microfluidic device for size-based cell separation by deterministic lateral displacement**

This figure shows the array of obstacles arranged in a staggered layout. The center-to-center distance between the obstacles is  $\lambda$  and the edge-edge distance between two obstacles is  $\delta$ . The obstacles are arranged in rows such that the center of any given obstacle is offset by a distance  $\Delta\lambda$  with respect to the corresponding obstacle in the previous row as shown in Figure 3. It is expected that, by manipulating and optimizing the obstacle parameters (spacing and diameter), as well as the staggering of each subsequent row of the patterned array, micron-sized particles can be sorted rapidly with high resolution. With 0.8-1.0  $\mu\text{m}$  beads, Huang et al achieved high resolution (within  $\sim 10\text{nm}$ ) separation within a short time ( $\sim 40\text{s}$ ). The resolution and speed of separation are controlled by manipulating  $\lambda$ ,  $\Delta\lambda$ , and  $v$  (the distance between rows of obstacles), and by using several different obstacle layouts in the same flow channel (as shown in Figure 3).

The total flux through each gap can be divided into  $n = 1/\varepsilon$  flow streams, where  $n$  is a whole number. The streams shift their positions cyclically so that after  $n$  rows, each streamline returns to its original position within the gap. Thus, for  $n = 3$ , streamline 1 moves to row 3 in the next row, to position 2 in the following row and back to position 1 after the third row (as indicated by the yellow arrows in the figure below).

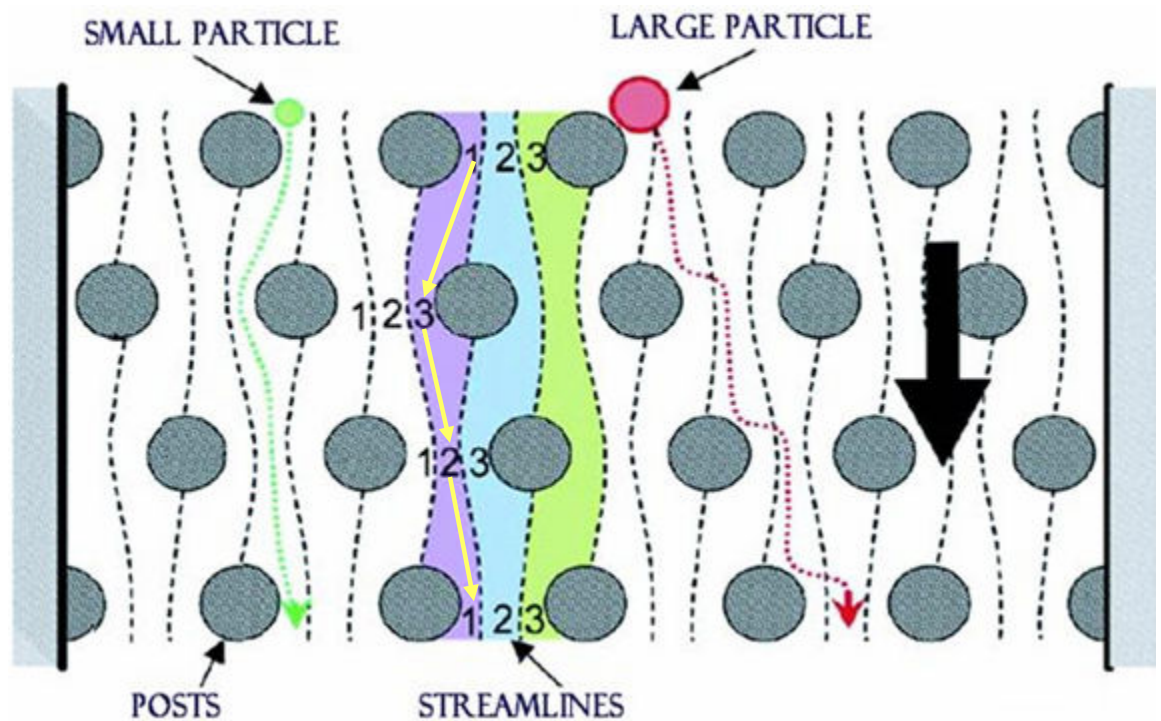


**Figure 4: Asymmetric bifurcation of spherical particles: size based separation where a stream of fluid flows perpendicular to a series of obstacles of defined size and spacing. The flow is confined to one of three fluid streamlines (denoted 1, 2, and 3). Particles smaller than the streamline width, zigzag between the obstacles. Larger particles collide with the obstacles and get displaced only in one direction, allowing for separation to occur [35].**

If a particle's radius is larger than the width of the streamline, the particle is laterally displaced near the post and coerced to remain in the higher numbered streamline as it crosses every row (displacement mode). Thus, the particle does not move parallel to the fluid flow but is at an angle determined by the ratio of the row offset to the center-center distance. Depending on the size of the particles in the stream and the obstacle parameters, the stream can enter one of two modes of displacement. If the width of the streamline is smaller than that of the particles, the particles follow the streamline and “zigzag” back and forth around the obstacles (zigzag mode). Particles smaller and larger than the critical diameter move in different directions and are thus sorted.

The parameters used in creating this model are defined as

$$\begin{aligned}\delta &= 2D_c \\ \varepsilon = \tan(\theta) &= \tan\left(\frac{\Delta\lambda}{\lambda}\right) \\ \lambda &= 5\delta\end{aligned}$$

$D_c$  is the critical diameter

$\delta$  is the edge to edge distance

$\theta$  is the angle of displacement expressed in arc degrees

$\lambda$  is the center to center distance

$\Delta\lambda$  is the row offset

The assumptions that were made in developing this model were that

- The fluid flow in the microfluidics device is limited to the plane holding the posts. The effect of the channel height on the flow profile has been neglected.
- The flow is laminar, viscous and time-invariant. Thus, the liquid moves in “layers”, without any mixing between the layers. Thus the particle follows the flow profile of the fluid and is moved at the same rate as the bulk fluid.
- Fluid flow in the microfluidic channels and between posts is fully-developed and the mean velocity is independent of position in the direction of flow.

This design was further developed and characterized by Inglis et al and was recently applied to the fractionation of whole blood into its components [35]. Davis and coworkers achieved 100% fractionation of the blood into erythrocytes, leukocytes, platelets, and plasma by size-based lateral displacement.

## 3.0 EXPERIMENTAL

### 3.1 Materials

Ethanol (200 proof), glass slides (35 x 60 mm, no. 1), microscope slides (25mm x 75mm, no. 5), 1mL graduated microcentrifuge tubes, Trypan Blue solution, and fetal bovine serum (FBS) were purchased from Fisher Scientific (Fair Lawn, NJ). (3,3,3-trifluoropropyl) trimethoxysilane was obtained from Gelest Inc. (Morrisville, PA). For device fabrication, SU-8 50 photoresist and developer were obtained from MicroChem (Newton, MA); silicone elastomer and curing agent were obtained from Dow Corning (Midland, MI). Phosphate buffered saline (PBS; 1x, without calcium or magnesium), RPMI and Dulbecco's Modified Eagle's Medium (DMEM) were purchased from Mediatech (Herndon, VA). Penicillin-Streptomycin (PS) and 0.25% trypsin/ethylene diaminetetraacetic acid (EDTA) solution in Hank's buffered salt solution (HBSS) (0.25% Trypsin-EDTA) were obtained from Hyclone (Logan, UT). The A7r5 rat aortic smooth muscle cell line and the H1975 human non-small lung cancer cell line were purchased from American Type Culture Collections (Manassas, VA). 3T3-J2 mouse embryonic FBs and H5V mouse capillary ECs were kindly provided by Dr. Yaakov Nahmias at the Massachusetts General Hospital and Dr. George Coukos at the University of Pennsylvania, respectively.

The steps involved in the process of device manufacture consists of spin coating, soft baking, exposure, post-exposure baking, developing, soft lithography and surface functionalization. The process parameters that have been optimized for this research work are described below.

## **3.2 Photolithography**

Photolithography is a process in microfabrication by which patterns on a semiconductor material can be defined using light. It uses light to transfer a geometric pattern from a photomask to a light-sensitive chemical (photoresist) on the substrate. The process involves 3 steps. First, a template design (photomask) is prepared. Next, the silicon wafer is coated with a chemical called a photoresist and finally, the template design is printed onto the chemically treated wafer to produce the master mold.

### ***3.2.1 Making the Photomask***

A photomask is a two dimensional projection of the pattern to be created on the device. The image for the mask originates from an AutoCAD data file. AutoCAD is useful for creating geometric features with a high degree of detail and complexity. These aspects make it a convenient tool for low-cost photolithography mask design. The image is then printed onto a transparent mylar plastic film using a photo-reproduction quality laser printer. Mylar masks are an inexpensive alternative to conventional chromium masks, for generating a transparency with geometries defined down to the tens of microns in resolution. The masks used in this work were designed to fit a 6-inch wafer and consisted of clear features on a dark background at 100 micron resolution. The printing of the masks was done by the photo plotting service bureau Fine Line Imaging.

### ***3.2.2 Photoresist Application***

The wafer was covered with SU-8 50 photoresist, which is a high contrast, epoxy based negative resist [37], by spin-coating. About 6ml of viscous liquid solution of

photoresist was dispensed onto the wafer, and the wafer was spun rapidly in the Brewer 100 CB Photoresist Spinner to produce a uniformly thick layer. The desired thickness of the SU-8 photoresist was achieved by controlling the spinning velocity. The spinner was ramped up to 500rpm at 100rpm/s for 5-10 seconds and then to 2500rpm at 300rpm/s for 30 seconds to produce a layer of an average thickness of 50 microns. The photoresist-coated wafer was subjected to a pre-bake step on a hot plate for 4 minutes at 65°C and for 10 minutes at 95°C to evaporate the solvent and harden the SU8 resist before exposure. Incrementing the temperature in steps ensures that the solvent evaporates at a slower rate resulting in good resist-to-substrate adhesion and high coating fidelity [38].

### ***3.2.3 Exposure and Developing***

The patterning of the photoresist was performed using the Quintel 4000-4 Contact Aligner. After pre-baking, the wafer was brought into contact with the mask and the pattern from the mask was replicated into the photoresist by ultraviolet illumination at 365 nm, 11 mW/cm<sup>2</sup>. After a brief post-bake step for 3 minutes at 65°C and for 7 minutes at 95°C, the unexposed photoresist was removed using SU-8 developer. As SU-8 is a negative photoresist, it becomes more robust due to cross-linking and is rendered insoluble to liquid solvents [37].

The cross-linking proceeds in two steps [37]:

1. Formation of a strong acid during the exposure process, followed by
2. Acid-initiated, thermally driven epoxy cross-linking during the post-exposure bake step

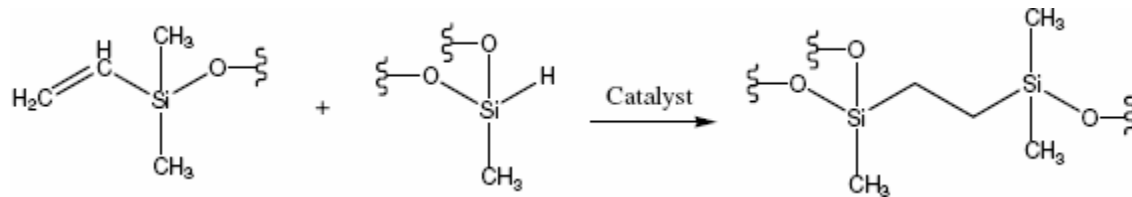
Thus the unexposed photoresist can be removed using SU-8 developer by agitation. After developing, the wafer was washed with isopropanol and dried. Appearance of a white precipitate indicates that the coating is underdeveloped and needs to be treated with SU-8 developer again [37]. The patterned features were verified using a Nikon Optiphot 200D microscope and the depth of the SU-8 coating was verified using a DekTak Profilometer 3ST. The patterned silicon wafer coated with the chemically and thermally stable SU-8 may thus be used as the master mold for the next step in device fabrication called ‘soft lithography’.

### **3.3 Soft Lithography**

Soft lithography represents a technique based on replica molding for carrying out micro- and nanofabrication. It provides a convenient, effective, and low-cost method for the formation and manufacturing of micro- and nanostructures. In soft lithography, an elastomeric stamp with patterned relief structures on its surface is used to generate patterns and structures with feature sizes ranging from 30 nm to 100  $\mu\text{m}$  [39].

The patterned silicon wafer was used as a mold to produce a PDMS replica. The SU-8 patterned 100 mm silicon wafer was secured onto a 150mm plastic petri dish with adhesive tape. The weight boat was sprayed with nitrogen gas to remove any particles and placed on the weighing scale. The pre-polymer base (vinyl-terminated PDMS) was

added to the curing agent (mixture of a platinum complex (catalyst) and copolymers of methylhydrosiloxane and dimethylsiloxane) in the weight ratio of 10:1. A plastic fork cleaned with isopropanol was used to mix the two reagents to a milky consistency. Mixing must be thorough since improper mixing may leave behind un-reacted curing agent with detrimental bonding results. The mixed PDMS was poured on top of the wafer fixed onto the petri dish. The petri dish cover was replaced and the whole assembly was transferred to a vacuum desiccator for the removal of air bubbles. The PDMS was degassed for at least 4 hours. The process of bubble disruption was hastened by intermittently releasing the vacuum and allowing air to rush in. The degassed PDMS assembly was then cured in an oven at 65°C for 24 hours. During the curing cycle, the liquid mixture becomes a solid, cross-linked elastomer due to the hydrosilylation reaction between vinyl (SiCH=CH<sub>2</sub>) groups and hydrosilane (SiH) groups [40].



After curing, the PDMS with the imprint was sectioned out using a standard surgical blade and peeled off the wafer which may be reused as a mold for the making the next PDMS replica.

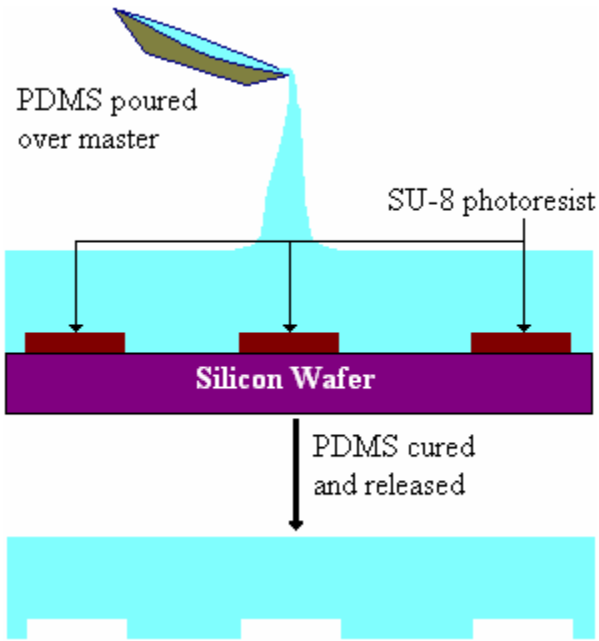


**Figure 5: Replica molding with PDMS**

Perforations were then made for the sample inlets and outlets using a sharpened syringe needle modified with a metal puncher fastened to the plunger. The fluid ports were made slightly larger than the outer diameter of the tubing used. The final device had features that are shown below in the figure.

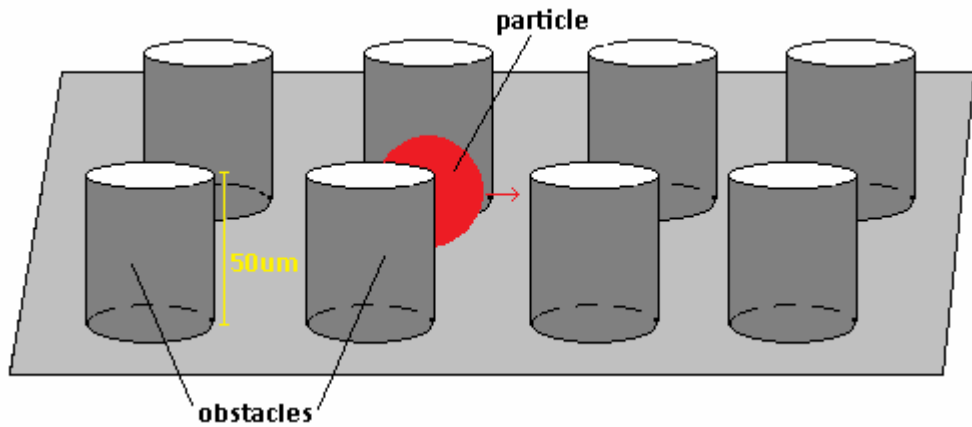


**Figure 6: Side view of a portion of the cylindrical post array used in microfluidic cell sorting post device**

### ***3.3.1 Properties of PDMS***

PDMS is a flexible elastomeric polymer that is well-suited for microfluidic device fabrication. Poly(dimethylsiloxanes) have a unique combination of properties resulting from the presence of an inorganic siloxane backbone and organic methyl groups attached to silicon [40]. They have very low glass transition temperatures ( $T_g \approx -125^\circ\text{C}$ ) and hence are fluids at room temperature [40]. These liquid materials can be readily converted into solid elastomers by cross-linking. The formulation, fabrication, and applications of PDMS elastomers have been extensively studied and are well-documented in the literature. The PDMS elastomer used in making this device also has other properties [40] that makes it useful in soft lithography:

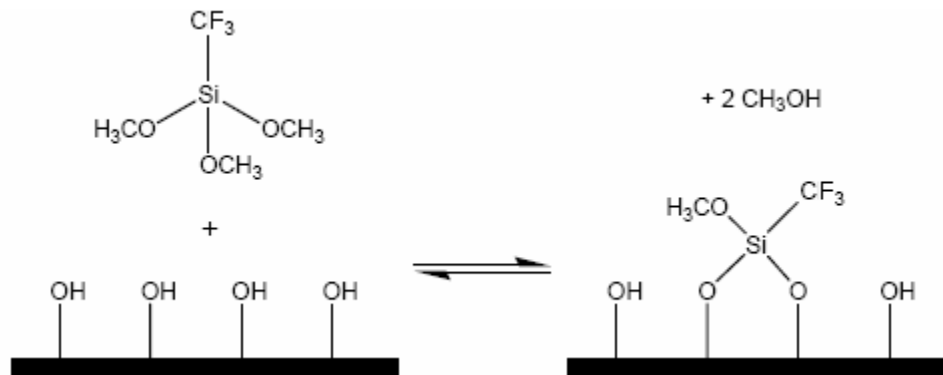
- a) The PDMS provides a surface that has a low interfacial free energy ( $\sim 21.6$  dyn/cm) and good chemical stability; most molecules or polymers being patterned or molded do not adhere irreversibly to, or react with, the surface of PDMS.
- b) The PDMS is not hygroscopic; it does not swell with humidity.
- c) The PDMS membrane is highly permeable to gases, which is important for maintaining cell viability.
- d) The PDMS elastomer has good thermal stability and thus can be used over a wide temperature range (at least from  $-50^\circ\text{C}$  up to  $+200^\circ\text{C}$  [41]); polymers being molded can be cured thermally.
- e) The PDMS elastomer is optically transparent down to  $\sim 300$  nm.
- f) The PDMS elastomer has unique flexural strength (shear modulus: 100 kPa - 3 MPa)
- g) PDMS has low chemical reactivity (except at extremes of pH levels), is non-toxic and biocompatible.

### 3.3.2. Surface Functionalization

A useful property of PDMS is that its surface can be chemically modified in order to obtain the interfacial properties of interest [39]. When PDMS is exposed to an oxygen plasma, it is covalently functionalized. Oxidation of the surface layer increases the concentration of hydroxyl groups and this leads to formation of strong intermolecular bonds. The polar silanol groups make the exposed surface highly hydrophilic.

PDMS replicas and glass slides were subjected to an oxygen plasma (100 mW, 8% oxygen, 30s exposure) in a PX-250 plasma chamber (March Instruments, Concord, MA). Oxygen Plasma is colorless but produced a violet color due to the presence of trace amounts of nitrogen or air. The devices were then immediately placed in contact to bond the surfaces irreversibly. The ambient humidity was maintained at ~40%. When silanol groups on PDMS are brought in contact with those on glass, a condensation reaction occurs resulting in the formation of Si-O-Si bonds forming a strong irreversible covalent bond (445 KJ/mol). The seal can withstand 30-50 psi of air pressure. The fluid pressure in microflows is  $\leq 6$  psi.

Immediately after the PDMS was bonded to the glass, the silanol surface was treated with a 4% (v/v) solution of (3, 3, 3-trifluoropropyl) trimethoxysilane in ethanol.



This treatment with fluorosilane increases the hydrophobicity of the glass and PDMS surfaces due to the presence of the highly electronegative fluorine atoms. This modification was done in order to alleviate the problem of cell adhesion to the devices surfaces while running the flow experiment.

### **3.4 Cell Culture**

H1975 cells were cultured in 75 cm<sup>2</sup> tissue culture flasks at 37°C in a humidified atmosphere with 5% CO<sub>2</sub> and 95% air. The cells were incubated in RPMI supplemented with 4.5 g/L glucose and L-glutamine, 10% FBS, 100 U/mL penicillin, and 100µg/mL streptomycin. Cells were grown to pre-confluence and isolated for experiments by trypsinization using a 0.25% Trypsin-EDTA solution. The cells were incubated at 37°C until the majority of cells get detached from the surface. The trypsinization was then terminated by addition of RPMI medium which contains trypsin inhibitor. 3T3-J2 fibroblast cells and H5V endothelial cells were similarly cultured in DMEM supplemented with L-glutamine, 10% FBS, 100 U/mL penicillin, and 100µg/mL streptomycin. Cells were grown to pre-confluence.

## 4.0 RESULTS AND DISCUSSION

The crucial difference between this method and the size-based sorting techniques used in earlier work is that it does not depend on diffusion or multipath averaging. Diffusion is critical in other devices applying asymmetric bifurcation to separate particles, as they depend on the random process of the particle to be able to diffuse far enough to be ratcheted by the obstacles. Thus these devices needed to be operated at low flow rates for diffusion effects to dominate, resulting in a slow separation protocol. This is in contrast to the deterministic lateral displacement technique which seeks to minimize diffusion effects, and improves with increasing flow rates. The flow rate is limited only by the shear force that the sample particles can withstand.

### 4.1 Wafer Fabrication

The devices constructed by Inglis et al [42] for blood fractionation were made of silicon with the pattern etched into wafers using a plasma etcher. The devices were sealed using PDMS coated glass slides. The technique used in this work does not require the etching process to be laboriously carried out for each individual device and instead uses soft lithography for cost-effective rapid prototyping, allowing the testing of several devices in a shorter time span. To create the master silicon mold, the SU-8 coated wafer with the overlaid photomask was exposed to the UV radiation for 20 seconds. When the wafer was baked and examined under the microscope it was observed that the posts were not fully formed- they were the expected size at the base, but tapered towards the top. It was suspected that the exposure time was insufficient.

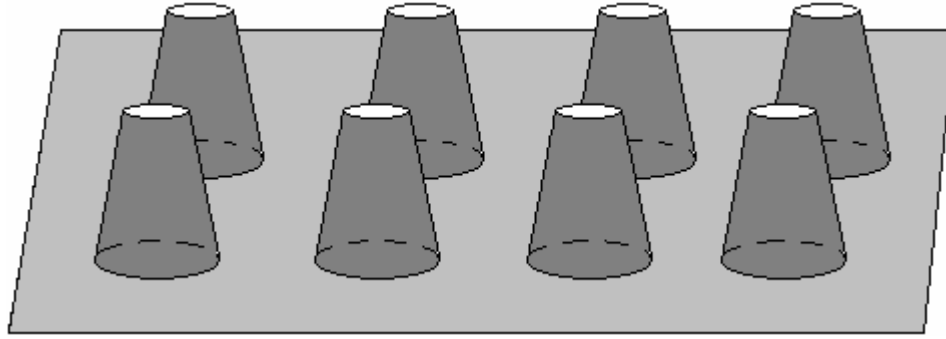


**Figure 7: Tapered structures formed due to insufficient exposure to UV radiation**

When the exposure time was increased to 40 seconds, it was observed that this resulted in posts with diameters larger than in the photomask. The technique was then modified as suggested by Mr Octavio Hurtado (BioMEMS Resource Center, Cambridge, MA). The optimized protocol was to expose the wafer to the UV light for 34 seconds in 2 second pulses at 10 second intervals. This resulted in well-formed features, with no change in dimensions. An additional flood exposure of the wafer to UV light for 40 seconds was used to harden the photoresist and improve the mechanical strength of the pattern. The patterned features on the wafer were verified using a Nikon Optiphot 200D microscope and the uniformity of the depth of the SU-8 coating was verified using a DekTak Profilometer 3ST.

The master silicon wafer was then used as a mold for pouring PDMS elastomer for soft lithography. Several faithful reproductions of the device pattern were produced by replica molding using PDMS. However, it was observed that, the quality of the devices deteriorated with usage as air bubbles remained trapped between the microscale features on wafer and the PDMS matrix. Degassing for longer periods of time and increasing the vacuum hastened the degassing process in the PDMS bulk, but it did not

help remove the air bubbles between the unpolymerized PDMS and the wafer features. High vacuum also caused the petridish to collapse. The quality of the devices may have been affected by surface tension changes after repeatedly treating the wafer with PDMS. The problem was not encountered with freshly made silicon master molds.

#### **4.2 Preparing the Cell Suspension**

The cells grown in the tissue culture flask were isolated by trypsinization. The medium was discarded and the cell monolayer was incubated at 37°C with 3ml of trypsin for 5-10 minutes. Once the majority of cells were detached (as observed under the microscope), the trypsinization was terminated by adding growth medium containing trypsin inhibitor. The cell suspensions was then centrifuged at 190 x g and then re-suspended in PBS to and adjusted to a concentration of  $0.5 \times 10^6$  cells/mL (measured using a hemacytometer under the microscope).

#### **4.3 Flow Experiments**

Two syringes containing the sheath fluid, PBS were fixed to a Harvard Apparatus PHD 2000 syringe pump (Holliston, MA). The device was connected to the two syringes through the tubing. The device inlets were initially purged of air bubbles by injecting PBS at a flow rate of 1ml/min. The syringe connecting the inlet for the cells was then refilled with cell suspension containing  $0.5 \times 10^6$  cells/ml. The flow rates for the fluid input to the device were standardized experimentally. The cell suspension was run at 40 $\mu$ l/min and the sheath fluid, PBS was run at 120 $\mu$ l/min. The cell movement was observed under a Nikon Eclipse TE2000-U microscope. At each outlet the volume of

suspension was determined and then the cell concentration was measured using a hemacytometer under the inverted microscope. The cell size distribution in the outlets was also measured by using the NIS elements software. The experiment was repeated for different sheath fluids (PBS, RPMI and serum-free RPMI) and the viability of the cells in the outlets collected was tested using the Dye Exclusion Method using the Trypan Blue stain. All experiments were performed at room temperature.

Experiments were conducted using cells suspended in PBS, serum-free medium and growth medium. Serum-free medium was tested as a sheath fluid in order to eliminate unpredictability of biological properties of serum batches [43]. However, it was observed that cell agglutination was high with PBS and serum-free media and reduced upon suspension in growth medium, possibly due optimum conditions for maintain cell integrity present in the growth medium. The duration of the experiment is short (~15min) but nevertheless there is a greater risk of cells undergoing replication while using growth medium, leading to erroneous data as cell size and shape can change during replication. Thus, to minimize this effect, the duration of the experiment must be made as short as possible.

#### **4.4 Device Design**

The goal of this design was to focus the majority of the cells in suspension to the top-most outlet (labeled “7”). As introduced by Huang et al [12], the device parameters are dictated by the diameter of the target cell. In this investigation, a non-small lung cancer cell line of diameter 15  $\mu\text{m}$  was used as a model cell line and only single cell suspensions were investigated.

The first version of the device is shown below.



**Figure 8: Initial device design**

This device consisted of an inlet for the sheath fluid and an inlet for the cell suspension. This device produced poor results since the inlet design does not persuade the cells to flow in a single file. The inlet was thus modified as shown in the figure below to enhance hydrodynamic focusing. The inlet was shifted to the corner of the device from the center in order to maximize the area of separation in the device.

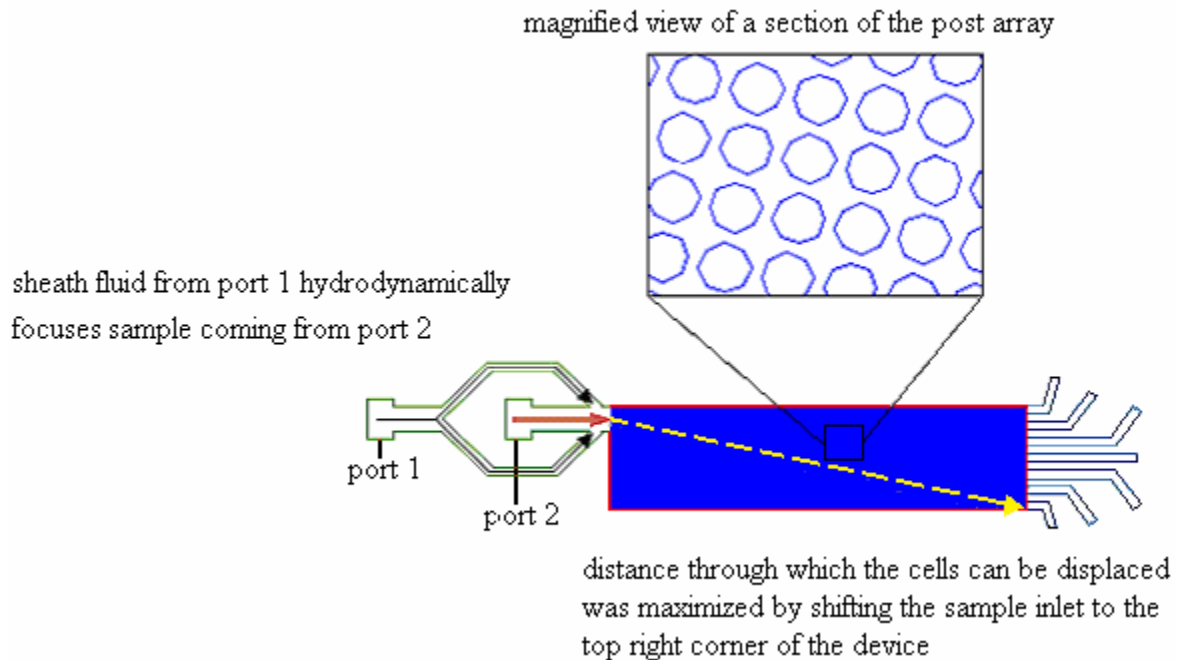


**Figure 9: Device design with modified inlet for hydrodynamic focusing of sample**

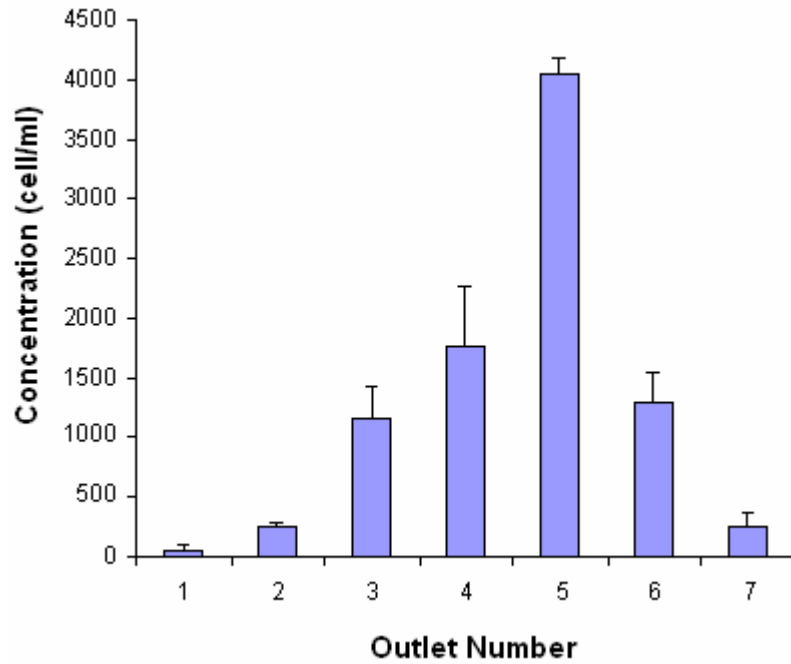


**Figure 10: H1975 cell concentration at each outlet. Outlet “1” is the bottom-most outlet and outlet “7” is the top-most outlet. An inlet concentration of  $0.5 \times 10^6$  cell/mL was injected into the device. Cells were focused to outlet “5” illustrating lateral displacement of target cells. Error bars denote standard errors for each point based on ten repetitions.**

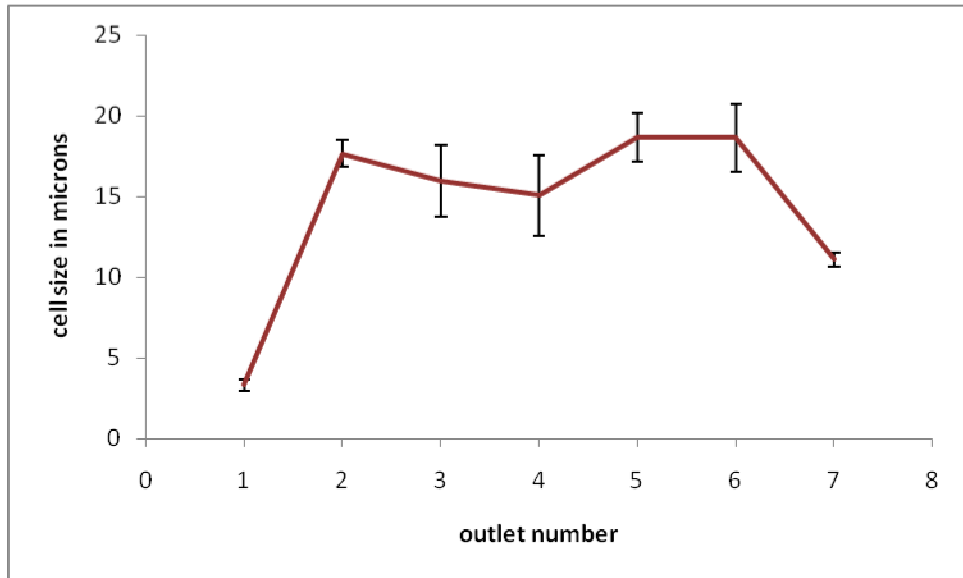


**Figure 11: The maximum concentration of cells was determined to be in the fifth position. These results illustrated the ability of the device design shown in Figure 5 to focus the cells to position “5”. It was determined by visual inspection that the displacement of the cells was occasionally hindered by the adhesion of cells between posts causing the streamline fluid flow to be displaced and thus the “bumping” of particles to be unpredictable and random.**

Several designs modifications were tested by altering the angle of the post array and the size of the gap between adjacent posts. One of the versions tested incorporated two regions with different critical diameters to improve the resolution of the device.

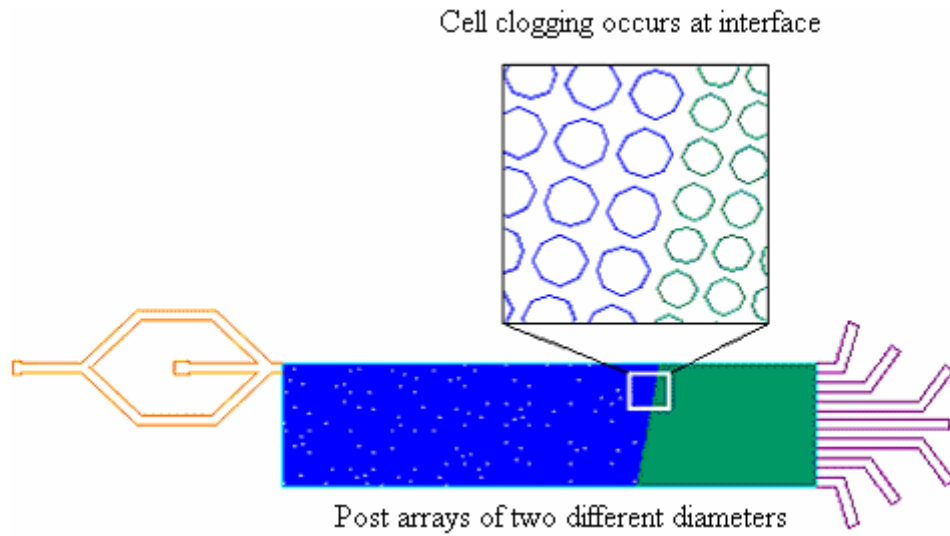


**Figure 12: Device design using two separation zones- larger posts (blue) are followed by smaller posts (green) downstream. A magnified view of the interface between both separation zones is shown.**

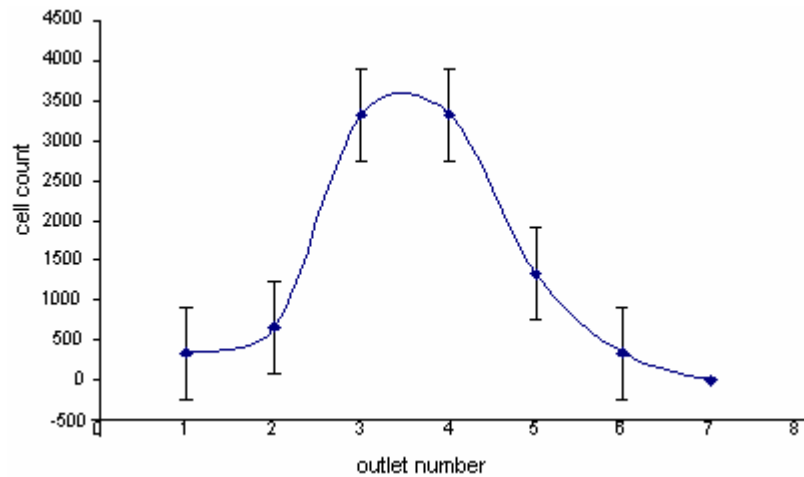


**Figure 13: H1975 cell fractions collected by using the device shown in figure 11 showed that the performance was significantly affected by the obstruction at interface. Error bars denote standard errors for each point based on three repetitions.**

The size and arrangement of the posts was determined by applying the same equations as described in Chapter 2. The problem encountered with this device was that particles would clog at the interface between the two regions and halted the experiment before complete processing of the sample.

The results from the most recent device design have been described below. The inlet was modified to create a hydrodynamically focused inlet stream of fluid. The inlet was shifted from the center to the extreme end in order to maximize the area available for cell separation. The posts were  $160\mu\text{m}$  in diameter; edge-edge distance was  $40\mu\text{m}$ ; the post array was angled at  $10^\circ$ . The entire device was about 2.5cm long and 1cm wide. The device consisted of a PDMS mold with patterned features bonded to a glass slide. The posts were  $\sim 50\mu\text{m}$  tall, which equals the maximum vertical space between the glass slide and the PDMS available for fluid flow.



**Figure 14: Final device design consisted of a longer separation zone to maximize the area available for cell movement**

The following figures describe cell size distributions (determined by hemacytometry) in the suspensions recovered from each of the seven outlets of the post-device shown in Figure 13. The device surface was functionalized using fluorosilane which mitigated the cell stiction in the device. H1975 cells have an average size of 20 microns size. Figure 15 shows that, while the first two channels and the sixth channel are

in line with our hypothesis, the seventh channel did not have the expected output of large sized cells. The device was designed by setting the critical diameter to 20 microns. Figure 16 shows the results obtained by using the same device with the A7r5 cell line. A7r5 cells have a size ~12 microns.

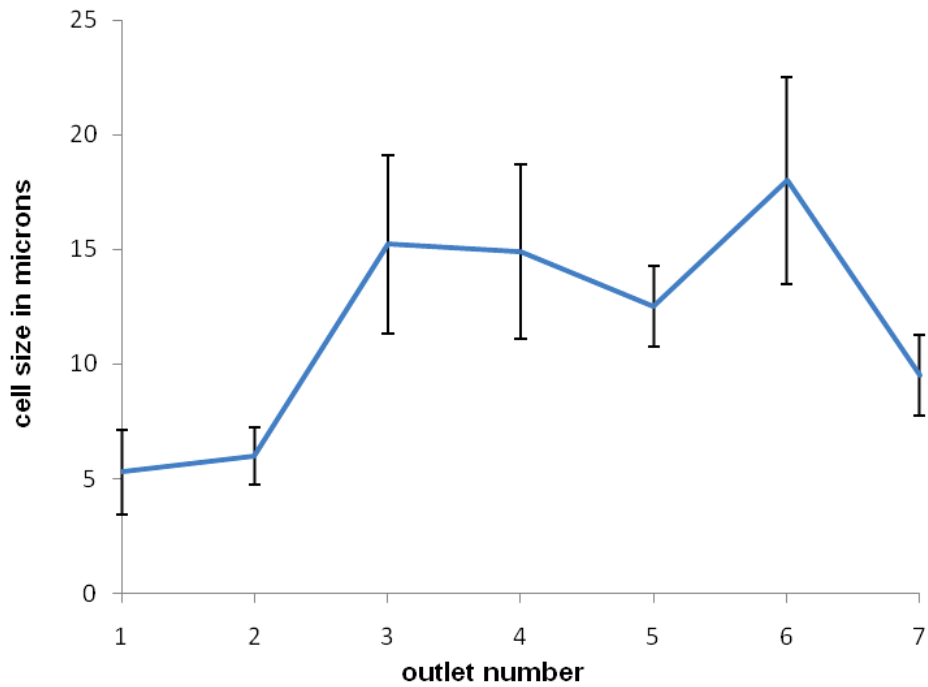


**Figure 15: Plot showing the size distribution of H1975 cells collected in each of the seven outlets. Error bars denote standard errors for each point based on ten repetitions.**

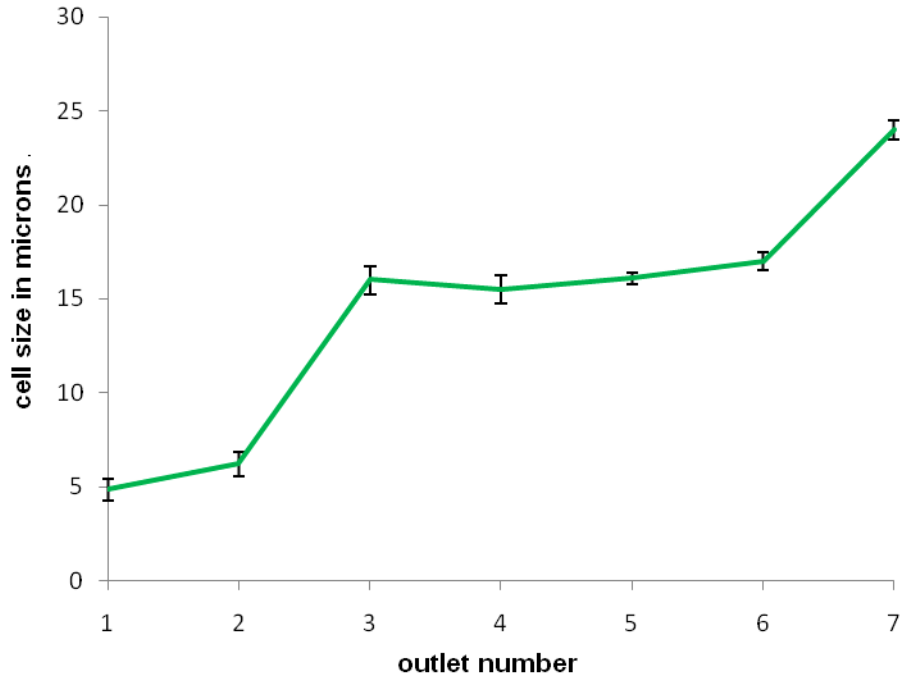


**Figure 16: Plot showing the size distribution of A7r5 cells collected in each of the seven outlets. Error bars denote standard errors for each point based on three repetitions**

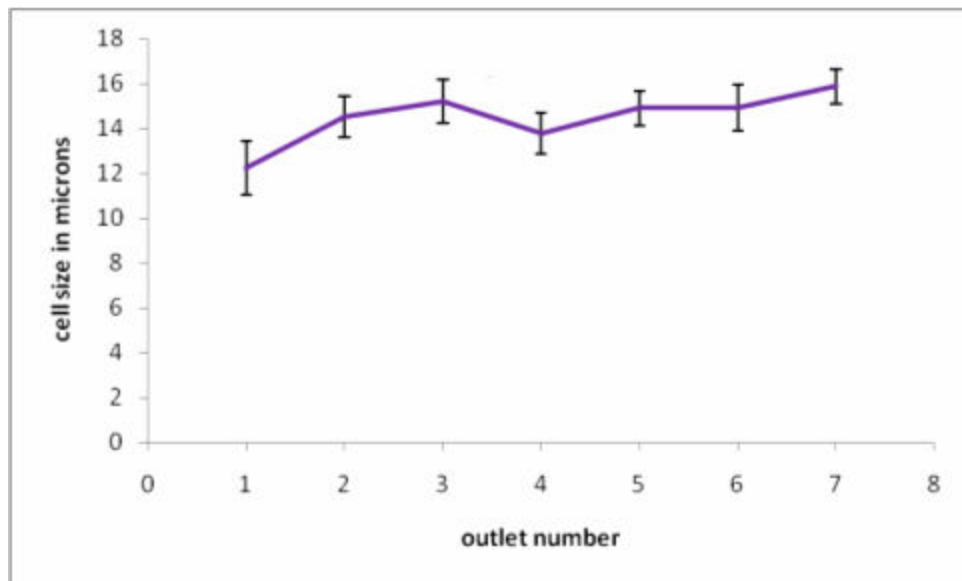


**Figure 17: Plot showing the size distribution of H5V fractions. Error bars denote standard errors for each point based on two repetitions**

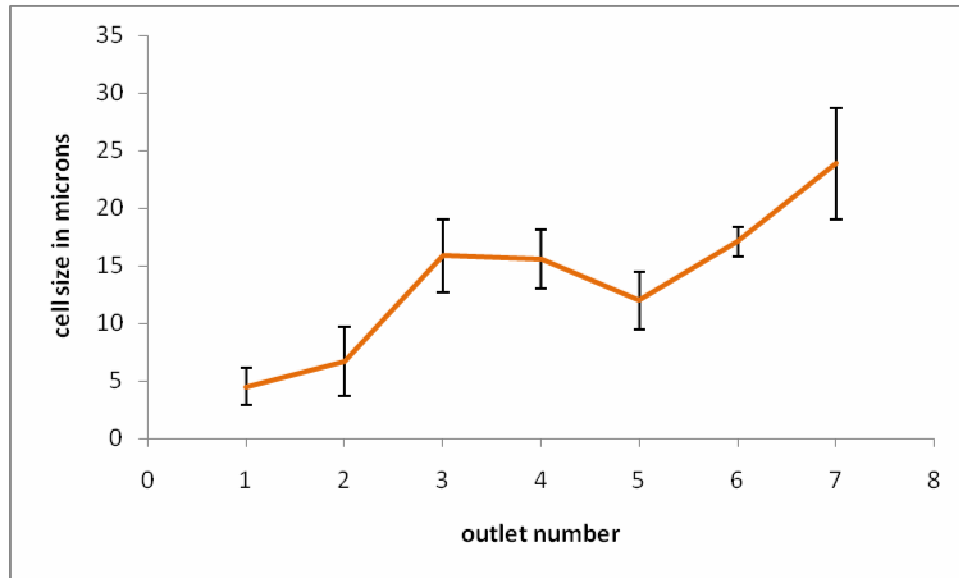


**Figure 18: Plot showing the size distribution of a1:1 mixture of H1975 cells and 3T3-J2 cells collected in each of the seven outlets. Error bars denote standard errors for each point based on two repetitions**

The dye exclusion tests proved that that ~90% of cells were alive in the samples collected. However, their viability needs to be confirmed by culturing the cell fractions collected at the output in growth medium. Flow experiments were also performed using spherical polystyrene beads in order to test the device using rigid particles in place of cells which are flexible. However it was observed that since these beads were more hydrophobic than the cells[44], they had a greater tendency to adhere to the device walls and the obstacles downstream.

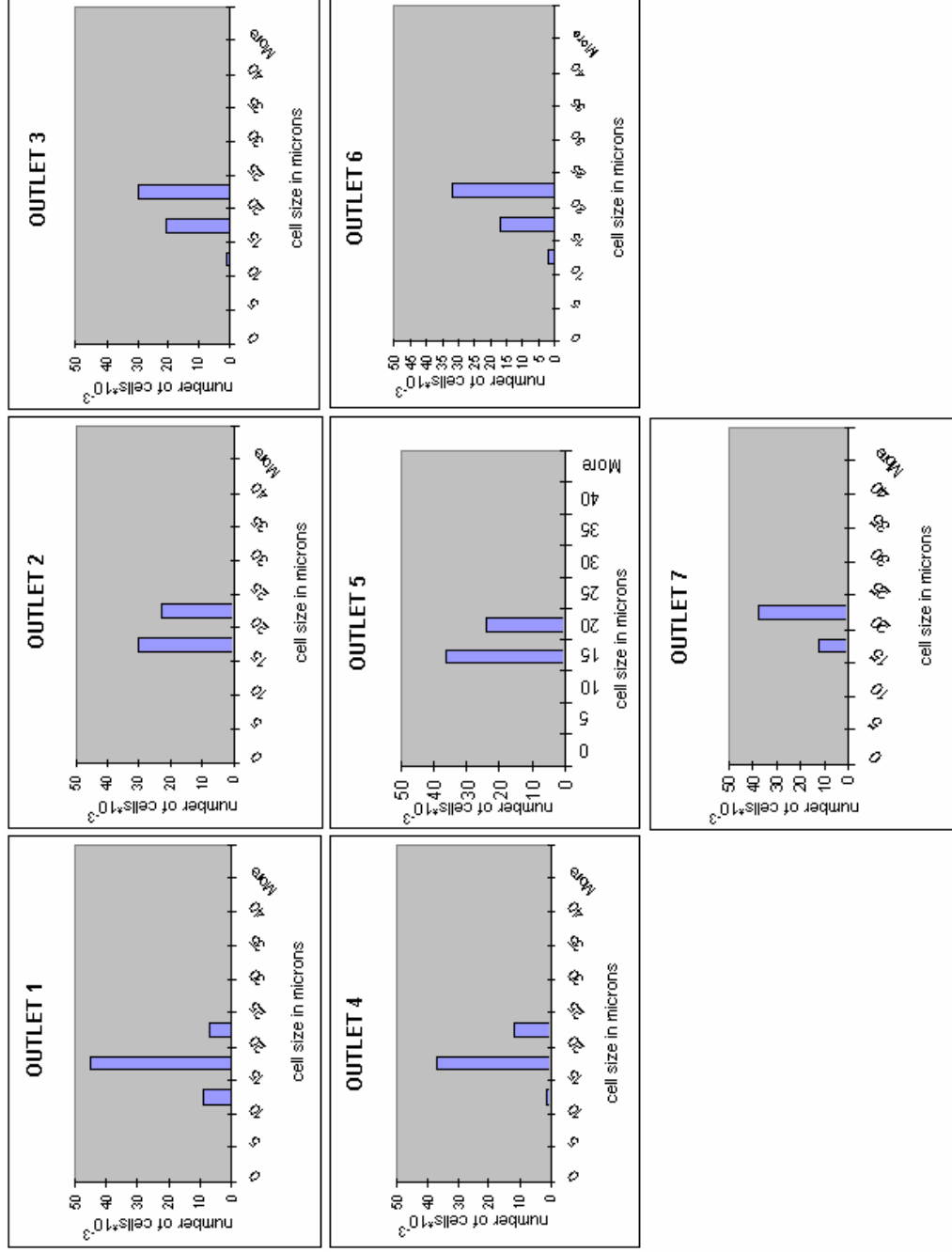


Figure 19: Size distribution of the cell fractions collected from seven outlets in a run conducted using H5V cells

## **4.5 Problems Encountered During Flow Experiments**

Some of the problems associated with the post-device flow experiments are as follows:

### ***4.5.1 PDMS Debris***

PDMS debris was formed while punching the inlet and outlet holes using a syringe if the PDMS matrix was too fragile. This caused the PDMS to get entrenched within the features within the device (see Figure 22). This was overcome to a large extent by standardizing the parameters for device fabrication. It was observed that even slight excesses of cross-linker and under-baking PDMS and caused the PDMS to break off while punching. The thickness of the PDMS layer poured did not have a significant impact on debris formation. In fact, if the PDMS is too thick, it becomes more difficult to punch smoothly and can lead to inlet and outlet holes that are less than perfect.

### ***4.5.2 Cell Stiction***

Towards the end of the test runs, it was observed that several cells expected to follow the streamline mode were found in the pathlines predicted to be taken by cells following the displacement mode. Cell stiction to the device surface broadens the cell separation profile and impairs device performance [45]. Fluorosilane treatment improved the hydrophobicity of the surfaces, but could not completely prevent the adhesion of cells to the posts and the walls of the device.

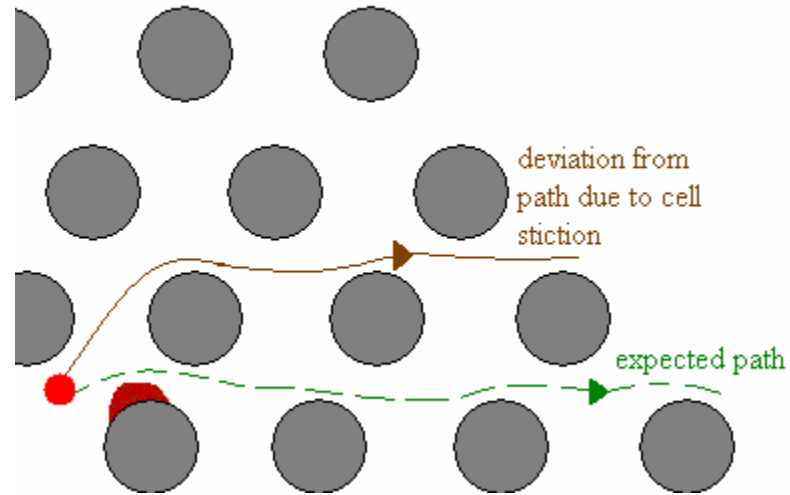


**Figure 20: Cell stiction disrupts flow pattern of cells**

It was also observed that the integrity of cells in the input sample was directly related to the freshness of the sample in line with the observation made by [45]. In samples that were run about 20 minutes after preparation, cells were found to aggregate near the entrance, and fibrous structures were observed, in a manner similar to the actin agglomeration phenomenon which is a precursor to cell death [46]. It was observed that a freshly prepared cell suspension (within ~5-10 min before flow experiment), maintained at a nominal concentration, prevents cells from forming clumps. Clumping causes erroneous results as small cells which would otherwise follow the streamline may form clumps and move as a unit and get laterally displaced downstream. Cell clumping was most pronounced at the inlet as was reported in literature [43].

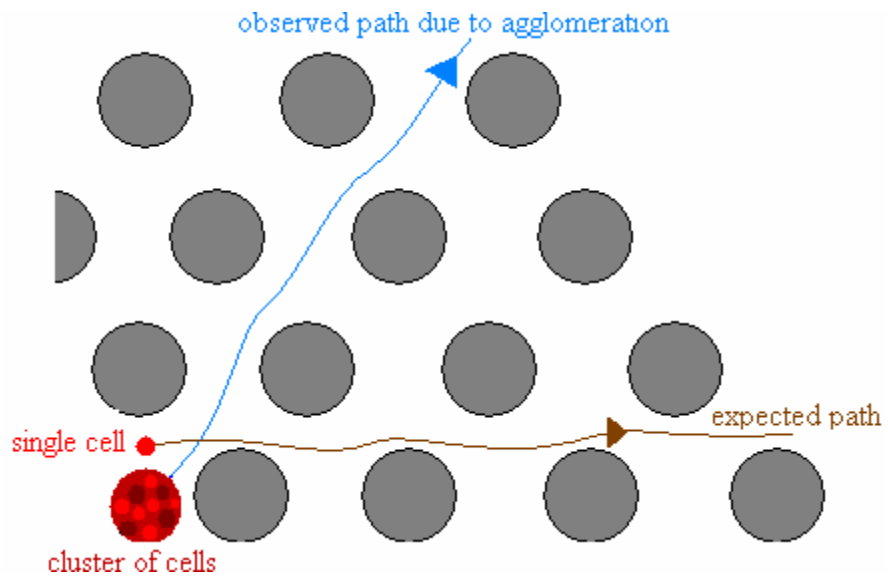


**Figure 21: Cell agglomeration causes smaller cells to form a larger unit and thus shifts the flow path away from the expected streamline**

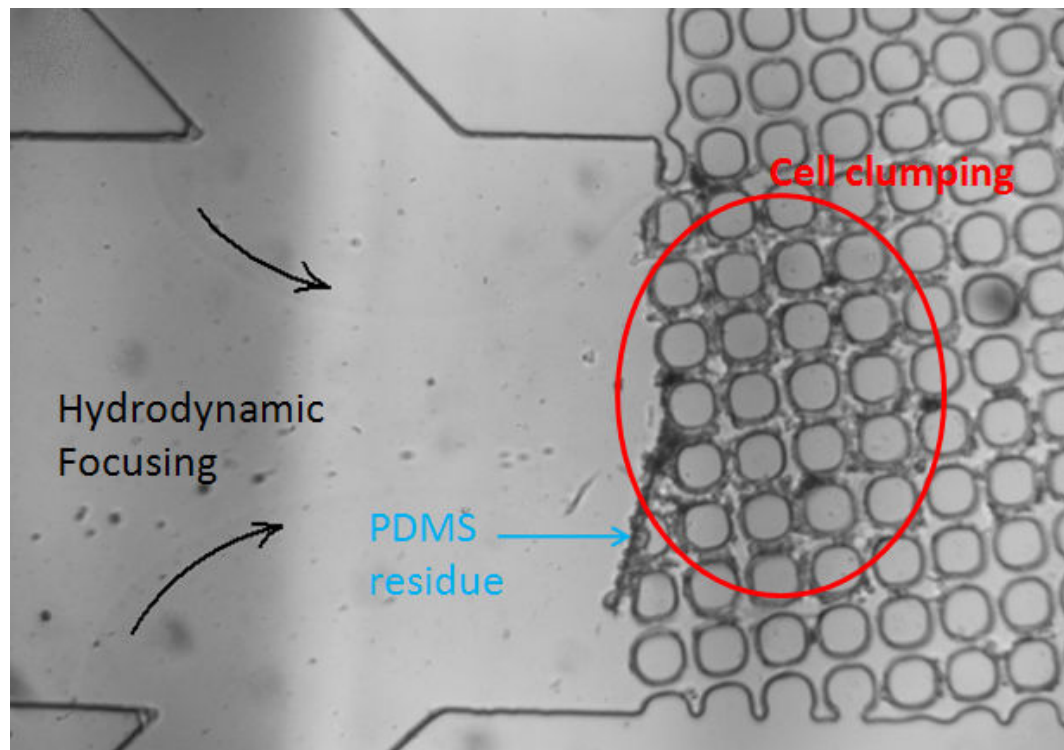


**Figure 22: Microscope image showing cell agglomeration near the entrance.**

It was also found that while running the flow experiments, cells often slipped through the gaps between posts due to their rather flexible structure.

Downstream, a small number of cells were also found to deviate from the expected pattern of lateral displacement as shown in Figure 13. The device design and flow parameters need to be adjusted in order to mitigate this problem.

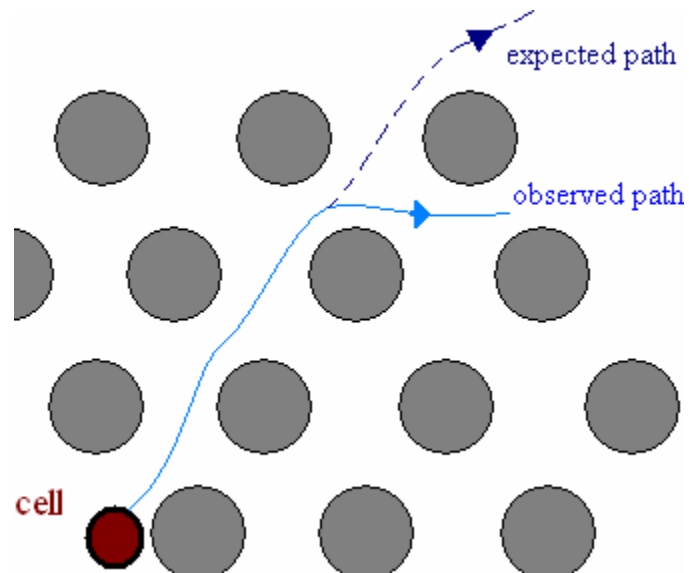


**Figure 23: Reverse displacement- cells are often disposed to move both ways around an obstacle**

## 5.0 CONCLUSIONS

The experiments with the microfluidic devices demonstrated that the technique of deterministic lateral displacement can be employed to fractionate a mixed cell suspension based on the sizes of the cells. Several post-device versions were fabricated and employed for cell isolation studies. The flow rates and inlet sample concentration were optimized. Experiments showed that this device could be useful, as hypothesized, for cell separation. However, several iterations of the device design must be performed, by varying different parameters before the device can be used for accurate separation of heterogeneous cell suspensions. The repeatability of the experiment proved to be low due to unpredictable cell behavior. There are a number of issues that require further studies for improving the performance of the post-device. The preliminary results for size-base cell separation have demonstrated the ability to enrich target cell populations, known to be of a large diameter, from a mixed cell suspension, with some success.

RPMI growth medium was found to be the most suitable sheath fluid for running the flow experiments. Fluorosilane treatment alleviated cell stiction to a perceptible extent. Wafer fabrication, device bonding and replica molding procedures were standardized. It was established that the freshness of the cell sample was a key factor in preventing cell clumping.

These findings suggest that the current design is a significant improvement over the earlier designs and could be capable of fractionating a cell sample containing several cell populations distinguished by size.

## 6.0 RECOMMENDATIONS

The results from the experiments conducted using microfluidic devices to sort cell suspensions using deterministic lateral displacement show that modifications must be made on several fronts improve the efficiency of the technique. The major problems associated with the performance of these devices is cell clumping, cell adhesion to the device surface, and cells straying into adjacent cell pathways thus decreasing resolution.

Future work would involve understanding the mechanisms of the above problems encountered while testing this device. The device performance can be simulated using a computer model by feeding in the device dimensions and flow parameters. The computer model would enable greater understanding of the deterministic lateral displacement technique, and modifying the design to counter phenomena observed in the device such as entrance effects, reverse displacement and diffusion, which negatively affect cell behavior within the device. The model was developed based on the assumption that flow between the posts is uniform and the particles do not affect the flow pattern due to their low density. A model incorporating parabolic instead of uniform velocity profile and particulate flow phenomena will enable a more realistic estimation of the theoretical performance of this device.

One of these approaches could be to re-evaluate the design parameters by applying the parabolic flow profile as the post size-gap ratio is increased. The current model assumes a uniform flow profile between posts. The critical diameter is dependent on the width of the streamline between the posts which is a variable in parabolic flow. According to Inglis et al, this effect can be factored in by including the variable parameter  $\eta$ . Thus the generalized formula for determining critical diameter is given by

$$D_c = 2\beta = 2\eta g \varepsilon$$

This reduces to the formula used in this thesis work when  $\eta = 1$  (uniform flow) and a post array slope of  $\varepsilon = 0.125$ . Thus by varying  $\eta$  and  $\varepsilon$ , a more accurate microfluidic device for separation by lateral displacement can be constructed.

Simulations performed using a design that includes more separation zones can improve resolution while fractionating a sample containing cell populations greatly differentiated by their size. The problem at the interface may be alleviated by applying the method used by Inglis et al[5], wherein the center-to-center distance is kept constant (instead of the post diameter as was in this research) and the post diameter to gap size ratio is varied

The next step would be to perform flow experiments with PDMS devices that incorporate the modifications made to eliminate these effects. In order to prevent clumping while using serum-free media, more experiments can be conducted by acclimatizing the cells to this medium instead of direct suspension in the medium as this could cause shock to the cells and hence death[43].

The integrity of the cell fractions collected can be confirmed by performing more authentic viability tests. If a means to perform the experiment in a sterile environment is developed, the cell fractions can be enriched by passaging the cells in a culture flask.

## 7.0 REFERENCES

1. Dupuy, A.M., S. Lehmann, and J.P. Cristol, *Protein biochip systems for the clinical laboratory*. Clin Chem Lab Med, 2005. **43**(12): p. 1291-302.
2. Plouffe, B.D., M. Radisic, and S.K. Murthy, *Microfluidic depletion of endothelial cells, smooth muscle cells, and fibroblasts from heterogeneous suspensions*. Lab Chip, 2008. **8**(3): p. 462-72.
3. Paegel, B.M., R.G. Blazej, and R.A. Mathies, *Microfluidic devices for DNA sequencing: sample preparation and electrophoretic analysis*. Curr Opin Biotechnol, 2003. **14**(1): p. 42-50.
4. Kang, L., et al., *Microfluidics for drug discovery and development: from target selection to product lifecycle management*. Drug Discov Today, 2008. **13**(1-2): p. 1-13.
5. Inglis, D.W., et al., *Determining blood cell size using microfluidic hydrodynamics*. Journal of Immunological Methods, 2008. **329**(1-2): p. 151-156.
6. Fortier, M.H., et al., *Integrated microfluidic device for mass spectrometry-based proteomics and its application to biomarker discovery programs*. Anal Chem, 2005. **77**(6): p. 1631-40.
7. Chaw, K.C., et al., *Multi-step microfluidic device for studying cancer metastasis*. Lab Chip, 2007. **7**(8): p. 1041-7.
8. de Mello, A., *Plastic fantastic?* Lab Chip, 2002. **2**(2): p. 31N-36N.
9. Beebe, D.J., G.A. Mensing, and G.M. Walker, *Physics and applications of microfluidics in biology*. Annu Rev Biomed Eng, 2002. **4**: p. 261-86.
10. Koepke, J.A., *Molecular Marker Test Standardization*. Cancer, 1992. **69**(6): p. 1578-1581.
11. Herzenberg, L.A., et al., *The history and future of the fluorescence activated cell sorter and flow cytometry: a view from Stanford*. Clin Chem, 2002. **48**(10): p. 1819-27.
12. Huang, L.R., et al., *Continuous particle separation through deterministic lateral displacement*. Science, 2004. **304**(5673): p. 987-90.
13. Situma, C., et al., *Fabrication of DNA microarrays onto poly(methyl methacrylate) with ultraviolet patterning and microfluidics for the detection of low-abundant point mutations*. Anal Biochem, 2005. **340**(1): p. 123-35.
14. Chao, T.C. and A. Ros, *Microfluidic single-cell analysis of intracellular compounds*. J R Soc Interface, 2008. **5 Suppl 2**: p. S139-50.
15. Radisic, M., R.K. Iyer, and S.K. Murthy, *Micro- and nanotechnology in cell separation*. Int J Nanomedicine, 2006. **1**(1): p. 3-14.
16. Rodriguez, W.R., et al., *A microchip CD4 counting method for HIV monitoring in resource-poor settings*. PLoS Med, 2005. **2**(7): p. e182.
17. Beltrami, A.P., et al., *Adult cardiac stem cells are multipotent and support myocardial regeneration*. Cell, 2003. **114**(6): p. 763-76.
18. Linke, A., et al., *Stem cells in the dog heart are self-renewing, clonogenic, and multipotent and regenerate infarcted myocardium, improving cardiac function*. Proc Natl Acad Sci U S A, 2005. **102**(25): p. 8966-71.
19. Oh, H., et al., *Cardiac progenitor cells from adult myocardium: homing, differentiation, and fusion after infarction*. Proc Natl Acad Sci U S A, 2003. **100**(21): p. 12313-8.
20. Orlic, D., et al., *Bone marrow cells regenerate infarcted myocardium*. Nature, 2001. **410**(6829): p. 701-5.
21. Bakhos, R., et al., *Comparative analysis of DNA flow cytometry and cytology of bladder washings: review of discordant cases*. Diagn Cytopathol, 2000. **22**(2): p. 65-9.

22. Albertsson, P.A., G. Johansson, and F. Tjerneld, *Separation processes in biotechnology. Aqueous two-phase separations*. Bioprocess Technol, 1990. **9**: p. 287-327.
23. Xuan, X. and D. Li, *Analytical study of Joule heating effects on electrokinetic transportation in capillary electrophoresis*. J Chromatogr A, 2005. **1064**(2): p. 227-37.
24. Laugwitz, K.L., et al., *Postnatal isl1+ cardioblasts enter fully differentiated cardiomyocyte lineages*. Nature, 2005. **433**(7026): p. 647-53.
25. Yamada, M., et al., *Microfluidic devices for size-dependent separation of liver cells*. Biomed Microdevices, 2007. **9**(5): p. 637-45.
26. Toner, M. and D. Irimia, *Blood-on-a-chip*. Annu Rev Biomed Eng, 2005. **7**: p. 77-103.
27. Zheng, S., Y.C. Tai, and H. Kasdan, *A Micro Device for Separation of Erythrocytes and Leukocytes in Human Blood*. Conf Proc IEEE Eng Med Biol Soc, 2005. **1**(1): p. 1024-1027.
28. Elimam, A., et al., *Diagnosis of hypoglycaemia: effects of blood sample handling and evaluation of a glucose photometer in the low glucose range*. Acta Paediatr, 1997. **86**(5): p. 474-8.
29. Nam-Trung Nguyen, S.T.W., *Fundamentals and Applications of Microfluidics*. 2002: Artech House. 471.
30. S. K. Sia, G.M.W., *Microfluidic devices fabricated in poly(dimethylsiloxane) for biological studies*. Electrophoresis, 2003. **24**(21): p. 3563-3576.
31. Westwood, S.M., et al., *Thick SU-8 and PDMS three-dimensional enclosed channels for free-standing polymer microfluidic systems*, in *Electrical and Computer Engineering, 2007. CCECE 2007. Canadian Conference on, IEEE*. 2007: Vancouver. p. 12-15.
32. Mohamed, H., et al., *Development of a rare cell fractionation device: application for cancer detection*. IEEE Trans Nanobioscience, 2004. **3**(4): p. 251-6.
33. Sethu, P., A. Sin, and M. Toner, *Microfluidic diffusive filter for apheresis (leukapheresis)*. Lab Chip, 2006. **6**(1): p. 83-9.
34. Shashi K. Murthy, P.S., Gordana Vunjak-Novakovic, Mehmet Toner, Milica Radisic, *Size-based microfluidic enrichment of neonatal rat cardiac cell populations*. Biomedical Microdevices, 2006. **8**: p. 231-237.
35. Davis, J.A., et al., *Deterministic hydrodynamics: taking blood apart*. Proc Natl Acad Sci U S A, 2006. **103**(40): p. 14779-84.
36. Giddings, J.C., *Field-flow Fractionation: Analysis of Macromolecular, Colloidal, and Particulate Materials*. Science, 1993. **260**: p. 1456-1465.
37. *Nano<sup>TM</sup> SU-8: Negative tone photoresist formulations 2002-2025*. 2002, Microchem Corporation.
38. Staff., M.C., *Nano<sup>TM</sup> SU-8: Negative tone photoresist formulations 2002-2025*. 2002, Microchem Corporation.
39. Xia, Y. and G.M. Whitesides, *Soft Lithography*. Angewandte Chemie, 1997. **37**(5): p. 550-575.
40. Clarson, S.J. and J.A. Semlyen, *Siloxane Polymers*. 1993: Prentice Hall 560.
41. *Sylgard<sup>TM</sup> 184 Silicone Elastomer Kit*. Dow Corning Corporation, 2005.
42. Inglis, D. and Princeton University. Dept. of Electrical Engineering., *Microfluidic devices for cell separation*. 2007, Princeton University, 2007. p. ix, 133 leaves.
43. *A Guide to Serum-Free Cell Culture*. 2003, Invitrogen Corporation.
44. *Polystyrene and Carboxylate-Modified Microparticles*. 1999, Thermo Scientific.
45. Zheng, S., et al., *Deterministic Lateral Displacement MEMS Device for Continuous Blood Cell Separation*. IEEE, 2005: p. 851-854.
46. Yang, S. and M.T. Saif, *Force response and actin remodeling (agglomeration) in fibroblasts due to lateral indentation*. Acta Biomater, 2007. **3**(1): p. 77-87.